Optogenetic stimulation of pre–Bötzinger complex reveals novel circuit interactions in swallowing–breathing coordination

Alyssa Huff[a] , Marlusa Karlen-Amarante[a] , Teresa Pitts[b], and Jan Marino Ramirez[a,c,1]

The coordination of swallowing with breathing, in particular inspiration, is essential for homeostasis in most organisms. While much has been learned about the neuronal network critical for inspiration in mammals, the pre–Bötzinger complex (preBötC), little is known about how this network interacts with swallowing. Here we activate within the preBötC excitatory neurons (defined as *Vglut2* and *Sst* neurons) and inhibitory neurons (defined as *Vgat* neurons) and inhibit and activate neurons defined by the transcription factor *Dbx1* to gain an understanding of the coordination between the preBötC and swallow behavior. We found that stimulating inhibitory preBötC neurons did not mimic the premature shutdown of inspiratory activity caused by water swallows, suggesting that swallow-induced suppression of inspiratory activity is not directly mediated by the inhibitory neurons in the preBötC. By contrast, stimulation of preBötC *Dbx1* neurons delayed laryngeal closure of the swallow sequence. Inhibition of *Dbx1* neurons increased laryngeal closure duration and stimulation of *Sst* neurons pushed swallow occurrence to later in the respiratory cycle, suggesting that excitatory neurons from the preBötC connect to the laryngeal motoneurons and contribute to the timing of swallowing. Interestingly, the delayed swallow sequence was also caused by chronic intermittent hypoxia (CIH), a model for sleep apnea, which is 1) known to destabilize inspiratory activity and 2) associated with dysphagia. This delay was not present when inhibiting Dbx1 neurons. We propose that a stable preBötC is essential for normal swallow pattern generation and disruption may contribute to the dysphagia seen in obstructive sleep apnea.

chronic intermittent hypoxia | rhythm generation | medullary circuitry

Breathing must continue throughout life, and many behaviors require strict coordination with breathing. Inhaled air drives vocalization (1, 2), and it is used to express emotions, such as crying and laughing (3). Respiratory muscles are used for cough production (4), and muscles activated during locomotion can facilitate respiration (5, 6). Even behaviors such as learning, memory, and arousal are linked to breathing and cardiorespiratory coupling (7, 8), and activity in the neocortex is in synchrony with respiratory activity (9, 10). Swallowing is an essential function found in mammals down to single-cell organisms (11–13). Mammals utilize 26 pairs of muscles across five cranial nerves, as well as cervical and thoracic segments of the spinal cord (14–17). Failure to coordinate swallowing with breathing can be fatal, and aspiration pneumonia associated with dysphagia is the leading cause of death in many disorders with respiratory impairments (18–21).

Swallowing–breathing coordination is complex, as there is considerable functional overlap. Some of the muscles have competing drive with respiratory activity and have multifunctional roles in swallowing and breathing (14, 15, 22). For example, the diaphragm is the major driver of inspiration, slows exhalation during postinspiration, and generates negative pressure for swallowing suction during schluckatmung. The anatomy is also multifunctional: food, fluid, and air share the same passage in breathing and swallowing, which requires complex coordination between the central nervous system and the peripheral nervous system (23). Swallowing can occur during any phase of breathing but usually follows inspiration occurring during postinspiration or expiration. This timing avoids ingestion during inspiration, decreasing the risk for aspiration. The timing is likely coordinated by inhibitory influences from the respiratory network on swallowing and from the swallowing network on inspiration.

The possibility to use optogenetic tools to activate specific neuron populations in defined brain regions in vivo allows for an in-depth interrogation of putative interactions between breathing and swallowing. There is considerable evidence that the inspiratory rhythm is generated in a specific region within the ventrolateral medulla, in the so-called pre–Bötzinger complex (preBötC) (24–27).

The preBötC is both sufficient and necessary for the generation of inspiration (24, 28–30). This rhythmogenic network is heterogenous, consisting of excitatory (glutamatergic) and inhibitory (glycinergic and gamma-aminobutyric [GABA]ergic) neurons

Significance

Swallowing is a vital behavior that must be coordinated with breathing. Both behaviors originate in the medulla, but the pathways responsible for their interactions have yet to be determined. It is hypothesized that inhibition from the medullary inspiratory driver, the pre–Bötzinger complex (preBötC), inhibits swallowing from occurring during times of inspiration. Using optogenetic stimulation of inhibitory and excitatory preBötC neurons, we provide evidence that the preBötC is involved in normal swallow production and coordination with breathing. We also suggest the preBötC is connected to the laryngeal motoneurons of the nucleus ambiguus (NA) and simulation of *Dbx1* neurons delays laryngeal closure, disrupting the normal swallow sequence. This study explores neural pathways involved in swallowing–breathing coordination.

Author affiliations: [a]Center for Integrative Brain Research, Seattle Children's Research Institute, Seattle, WA 98101; [b]Department of Neurological Surgery, School of Medicine, University of Louisville, Louisville, KY 40202; and [c]Department of Neurological Surgery, School of Medicine, University of Washington, Seattle, WA 98108

(26, 28, 31–35). Critical for rhythmogenesis is a subset of glutamatergic neurons that is derived from precursors expressing the transcription factor developing brain homeobox 1 protein (*Dbx1*) (36–39). By specifically activating inhibitory and excitatory neurons in the preBötC during water-evoked swallows, we evaluated how each of these neuron types affects swallow behavior in a freely breathing anesthetized mouse preparation.

We expect that manipulating the activity of these neurons will provide insights into the interactions between inspiratory activity and swallowing. Swallowing is thought to be generated by a swallow pattern generator comprised of two distinct neuronal groups: the dorsal swallow group (DSG) in the dorsomedial medulla and the ventral swallow group (VSG) in the ventrolateral medulla (40). The DSG is thought to be located within, but not limited to, various subnuclei within the nucleus tractus solitarii (NTS) (40–42), and it receives vagal and spinal afferent information from the airway and thoracic regions, shaping the swallow response. Premotoneurons within the swallow-related subnuclei of the NTS have known projections to pharyngeal motoneurons in the semicompact nucleus ambiguus (NA), laryngeal motoneurons in the loose-formation NA, and esophageal motoneurons in the compact-formation NA (43–45). The VSG contains pharyngeal and laryngeal motoneurons within and around the NA (44) that are thought to be responsible for the switching and precise coordination of swallow-related and presumed respiratory-related muscles (40, 42). However, the precise role of the VSG in swallow behavior is unknown, as are the neuronal and modulatory mechanisms that coordinate swallowing- and breathing-related neural circuitry.

Respiratory conditions that cause chronically altered blood gases result in significant alterations in swallowing–breathing coordination, with the majority of swallows occurring during inspiration. This leads to the common problem of dysphagia in patients with obstructive sleep apnea (OSA) (46), and chronic obstructive pulmonary disease (COPD) (47, 48). To further understand the mechanisms of swallowing–breathing coordination, we compared interactions in chronic exposure of intermittent hypoxia. Chronic intermittent hypoxia (CIH) decreases excitability in the preBötC, resulting in irregular frequency and amplitude of the inspiratory rhythm, as well as failed hypoglossal transmission (49).

We hypothesize that modulation of the preBötC will alter swallow pattern generation and coordination with breathing. Our study, which combines optogenetic manipulation in an in vivo preparation with water-evoked swallowing, sheds light on the importance of a stable inspiratory network on swallow motor pattern and coordination with breathing.

Results

The preBötC is a heterogenous network that contains inhibitory and excitatory neurons, as well as a subset derived from the precursors that express the transcription factor *Dbx1* (36–38). Here we differentially activated inhibitory and excitatory neurons in the preBötC and then more specifically the *Dbx1* neurons in the preBötC to gain understanding of circuit-level interactions between the preBötC and swallow behavior. *SI Appendix,* Tables S1–S3 shows descriptive statistics of all swallow-related parameters.

Decrease in Drive for Breathing and Increase in Swallow Drive Delays Subsequent Inspiration.
Optogenetic stimulation of Vgat neurons within the preBötC. To understand the interaction of inhibitory neurons in the preBötC and swallowing, we optogenetically stimulated *Vgat* neurons using *Vgat*cre[Ai32] mice ($n = 10$). We found a significant increase in the interburst interval of the diaphragm (from 787 ± 189 to $1,062 \pm 329$ ms, $P = 0.02$) and inspiratory delay (from 292 ± 114 to 542 ± 203 ms, $P = 0.01$) during preBötC stimulation of *Vgat* neurons (Fig. 1). All 10 animals swallowed in response to water before and during *Vgat* stimulation; however, swallow number decreased significantly (from 5 ± 2 to 3 ± 2, $P = 0.05$) during stimulation.

Under baseline control conditions, 13% of swallows were identified as having a schluckatmung, i.e., swallows that were characterized by the concurrent activation of diaphragmatic activity. During preBötC *Vgat* stimulations, there were zero occurrences of schluckatmung activity.

Increase in Drive for Both Breathing and Swallowing Causes Delay in Swallow-Related Laryngeal Closure.
Optogenetic stimulation of Vglut2 neurons within the preBötC. In control animals, bilateral stimulation of *Vglut2* neurons within the preBötC in *Vglut2*cre[Ai32] mice ($n = 10$) significantly increased swallow-related integrated XII nerve amplitude (from 81 ± 11 to 105 ± 34% of maximum, $P = 0.03$) and X nerve amplitude (from 75 ± 16 to 93 ± 28% of maximum, $P = 0.03$) (Fig. 2A). The duration of swallow-related laryngeal complex activity increased during *Vglut2* stimulation of the preBötC (from 305 ± 147 to 372 ± 205 ms, $P = 0.05$). This caused the inspiratory delay to significantly decrease (from 506 ± 431 to 210 ± 138 ms, $P = 0.05$). The number of swallows did not change during *Vglut2* stimulation. In contrast to stimulation of *Vgat* neurons, we observed no change in the prevalence of schluckatmung during stimulation of *Vglut2* neurons within the preBötC.
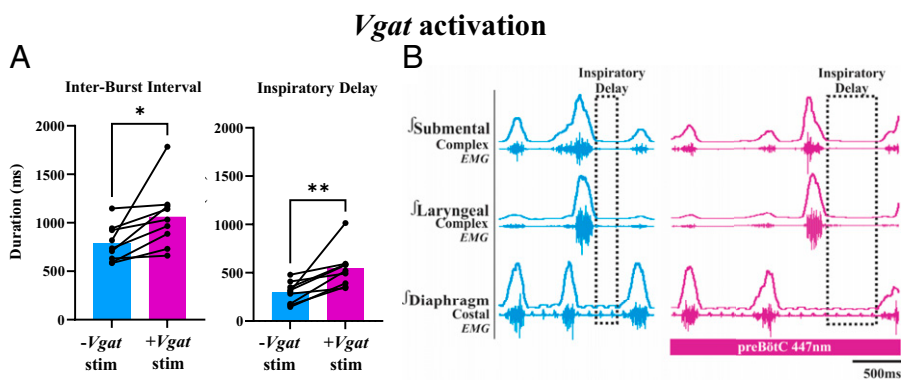
Vgat activation

Fig. 1. Optogenetic stimulation of inhibitory *Vgat* neurons does not disrupt swallow pattern but instead delays the next inspiratory cycle in control mice. (*A*) Bar graph showing a significant increase in the average swallow-related diaphragm interburst interval and inspiratory delay when *Vgat* neurons are activated (purple) in control mice. Each black dot represents one animal (mean ± SD, P = 0.02, P = 0.01, n = 10). (*B*) Representative traces of what is depicted in *A*, with the black dotted rectangle showing inspiratory delay duration in both traces. Blue is a baseline swallow and purple is a swallow induced during *Vgat* stimulation.
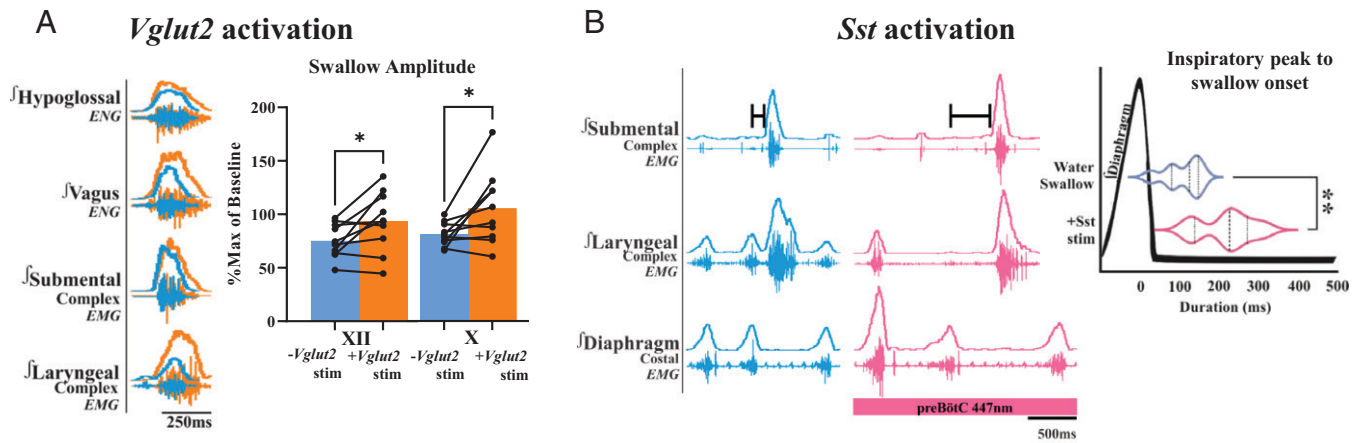
Fig. 2. Optogenetic stimulation of excitatory neurons either increases swallow amplitude (*Vglut2*) or alters swallowing–breathing coordination (*Sst*). (*A*) Representative trace of control swallow (blue) and water swallow induced during *Vglut2* stimulation (orange). Bar graph showing a significant increase in swallow-related hypoglossal and vagus amplitude, with each dot representing one animal cycle (mean $\pm$ SD, $P = 0.03$, $P = 0.03$, $n = 10$). (*B*) Representative trace of control swallow (blue) and water swallow induced during *Sst* stimulation (pink). The violin plot demonstrates swallow occurrence significantly later in the respiratory cycle. The dark dotted line depicts the average time a swallow occurs in relation to peak diaphragm activity (mean $\pm$ SD, $P = 0.001$, $n = 7$), with no change in interburst interval ($P = 0.09$) or inspiratory delay ($P = 0.74$) (as defined in Fig. 6).

Optogenetic stimulation of *Sst* neurons within the preBötC. In control animals, bilateral stimulation of *Sst* neurons within the preBötC in *Sst*cre^{Ai32} mice ($n = 7$) significantly delayed swallow onset in relation to peak diaphragm activity (from 109 ± 46 to 219 ± 69 ms, $P = 0.001$) (Fig. 2*B*). Swallow number and prevalence of schluckatmung did not change during stimulation of *Sst* neurons within the preBötC.

Optogenetic stimulation of *Dbx1* neurons within the preBötC. Optogenetic activation of *Dbx1* neurons within the preBötC in *Dbx1*cre^{Ai32} animals ($n = 7$) increased the oropharyngeal sequence, delaying laryngeal closure (from 21 ± 33 to 99 ± 77 ms, $P = 0.04$, one-tailed *t* test) (Fig. 3*A*). During baseline conditions, nine animals swallowed in response to water-induced swallow stimulation; however, during activation of *Dbx1* neurons

within the preBötC, two of the animals lost their swallow response, removing them from our analysis. The average number of swallows per animal was reduced by 50%, although this was not significant. Prevalence of schluckatmung during *Dbx1* activation of preBötC was not altered.

Optogenetic inhibition of *Dbx1* neurons within the preBötC. Optogenetic inhibition of *Dbx1* neurons within the preBötC in *Dbx1*cre^{Ai40D} animals ($n = 4$) increased laryngeal complex duration (from 190 ± 24 to 218 ± 23 ms, $P = 0.04$) and swallow-related inspiratory delay (from 299 ± 61 to 331 ± 63 ms, $P = 0.03$) (Fig. 3*B*). Neither the number of swallows nor the prevalence of schluckatmung changed during *Dbx1* inhibition.

CIH Causes Delay in Swallow-Related Laryngeal Closure. CIH has been associated with dysphagia (50, 51), and this study
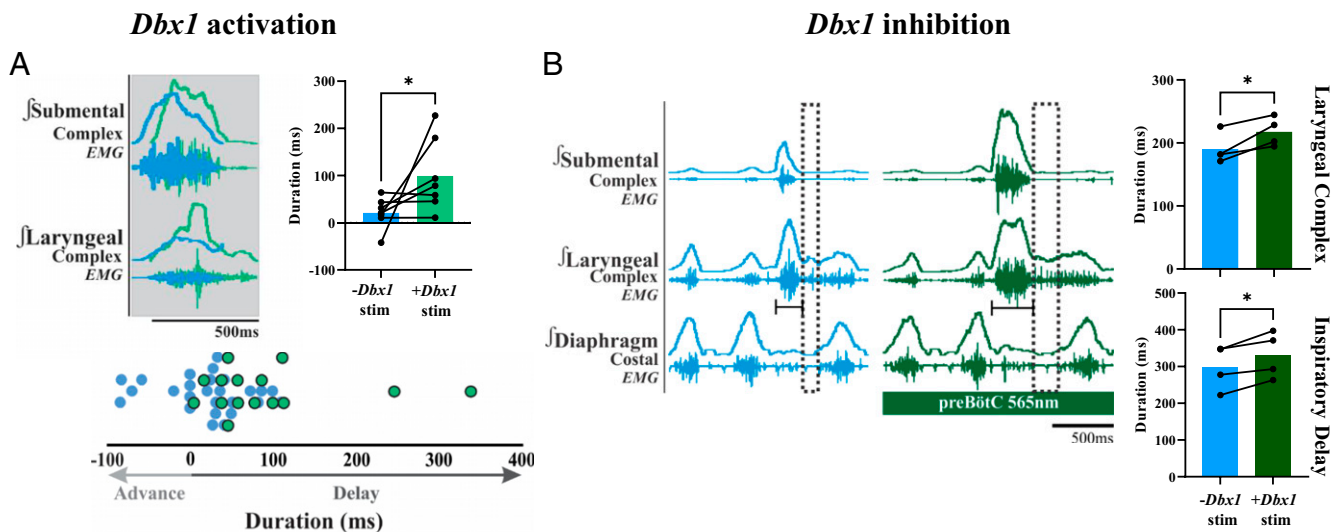

Fig. 3. Optogenetic stimulation of *Dbx1* neurons delays laryngeal closure, while optogenetic inhibition delays the subsequent inspiratory burst. (*A*) Representative trace of a baseline swallow (blue) overlayed with a swallow induced during *Dbx1* stimulation (light green), showing the delay of peak laryngeal complex activation. The bar graph to the right quantifies what is shown in the representative trace, with each black dot representing one animal (mean $\pm$ SD, $P = 0.04$, one-tailed *t* test, $n = 7$). The bottom dot plot is pooled data, showing the time delay/advance of the swallow sequence, with each dot representing a single swallow. Light green shows the decreased number of swallows during *Dbx1* stimulation. (*B*) Representative trace of a baseline swallow (blue) and a swallow induced during *Dbx1* inhibition (dark green), showing the increased swallow-related laryngeal complex duration and delay of the subsequent inspiratory burst (dotted black rectangle). This effect appears to be similar to swallows with targeted superior laryngeal nerve stimulation (80). Bar graphs to the right quantify what is shown in the representative trace, with each black dot representing one animal. Laryngeal complex duration (mean $\pm$ SD, $P = 0.04$, $n = 4$) and inspiratory delay (mean $\pm$ SD, $P = 0.03$, $n = 4$) are shown.
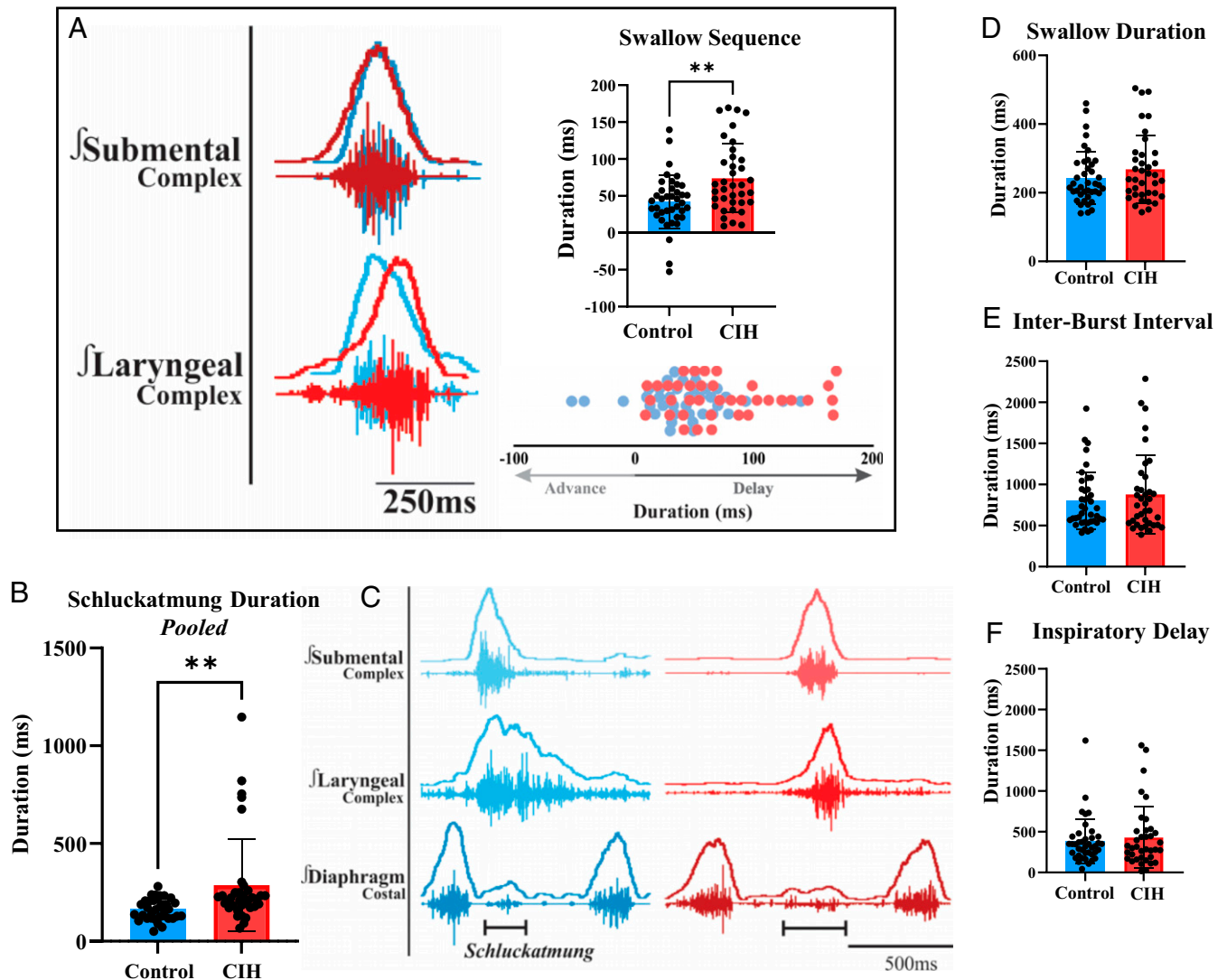
Fig. 4. CIH causes the same phenomenon as observed during *Dbx1* stimulation (Fig. 3*A*). (*A*) Left is a control swallow (blue) and a CIH-exposed swallow (red) showing delay in laryngeal complex peak activation. The top right quantifies what is shown in the trace (mean ± SD, P = 0.001, n = 40, 37, respectively, mean ± SD), and below is the delay in milliseconds, with each dot representing one animal. (*B*) Since schluckatmung (swallow-related diaphragm activity) does not occur in every animal, we pooled the data for every swallow with its occurrence. Schluckatmung duration is significantly increased in animals exposed to CIH (mean ± SD, P = 0.003). (*C*) Representative traces of what is shown in *B*. The black bar at the bottom depicts schluckatmung duration. (*D–F*) CIH exposure did not change swallow duration, the swallow-related (SR) diaphragm interburst interval, or the SR inspiratory delay.

characterizes swallows in mice exposed to CIH. In observing control (n = 40) and CIH (n = 37), we found a significant delay in swallow-related laryngeal closure, mimicking what is seen during *Dbx1* stimulation (Fig. 4*A*). The average delay in control animals was 42 ± 36 ms and in CIH was 74 ± 47 ms (P = 0.001). Pooled data from all swallows containing schluckatmung activity showed a significantly longer diaphragm duration after CIH exposure (163 ± 54 versus 287 ± 234 ms, P = 0.003) (Fig. 4*B* and *C*). Under control conditions, 15% of swallows had schluckatmung, while CIH-exposed animals increased to 19% of swallows. We saw no significant change in swallow duration, swallow-related expiratory duration, or inspiratory delay between control and CIH conditions (Fig. 4*D–F* and [SI Appendix](#), Table S2). We also found that mice exposed to CIH weighed significantly less than control mice (25 ± 4 versus 20 ± 3 g, P = 0.0001).

Respiratory phase-shift plots demonstrate the influence of swallow activity on the respiratory rhythm (Fig. 5*A*). In control conditions, swallows that occurred during inspiration did not reset the respiratory cycle, except in some cases when the next cycle was advanced, occurring sooner than the previous expected phases. For the swallow activity occurring during postinspiration and later stages of expiration, the next inspiratory burst was delayed in proportion to the swallow activity. The swallowing–breathing phase relationship became less predictable in animals exposed to CIH. Moreover, there were many more incidences of swallows occurring during inspiration that resulted in a delayed inspiratory burst, as well as a greater delay in the next inspiratory burst when swallowing occurred during postinspiration and into later stages of expiration. Fig. 5*B* shows a residual plot demonstrating the absolute distance at which each point falls in relation to the line of best fit from Fig. 5*A*. A test of means on the residual revealed a significant difference in CIH compared to control animals (P = 0.007).

We categorized each swallow as either normal—control or CIH—or atypical to explore if any of the nonclassic, atypical swallow-related activities resulted in phase-resetting changes. Atypical swallows included swallows containing schluckatmung, swallow causing an abrogated inspiratory burst and swallow containing both schluckatmung and abrogated inspiratory burst (Fig. 6*C*). Fig. 5*A* shows normal or atypical swallow activity
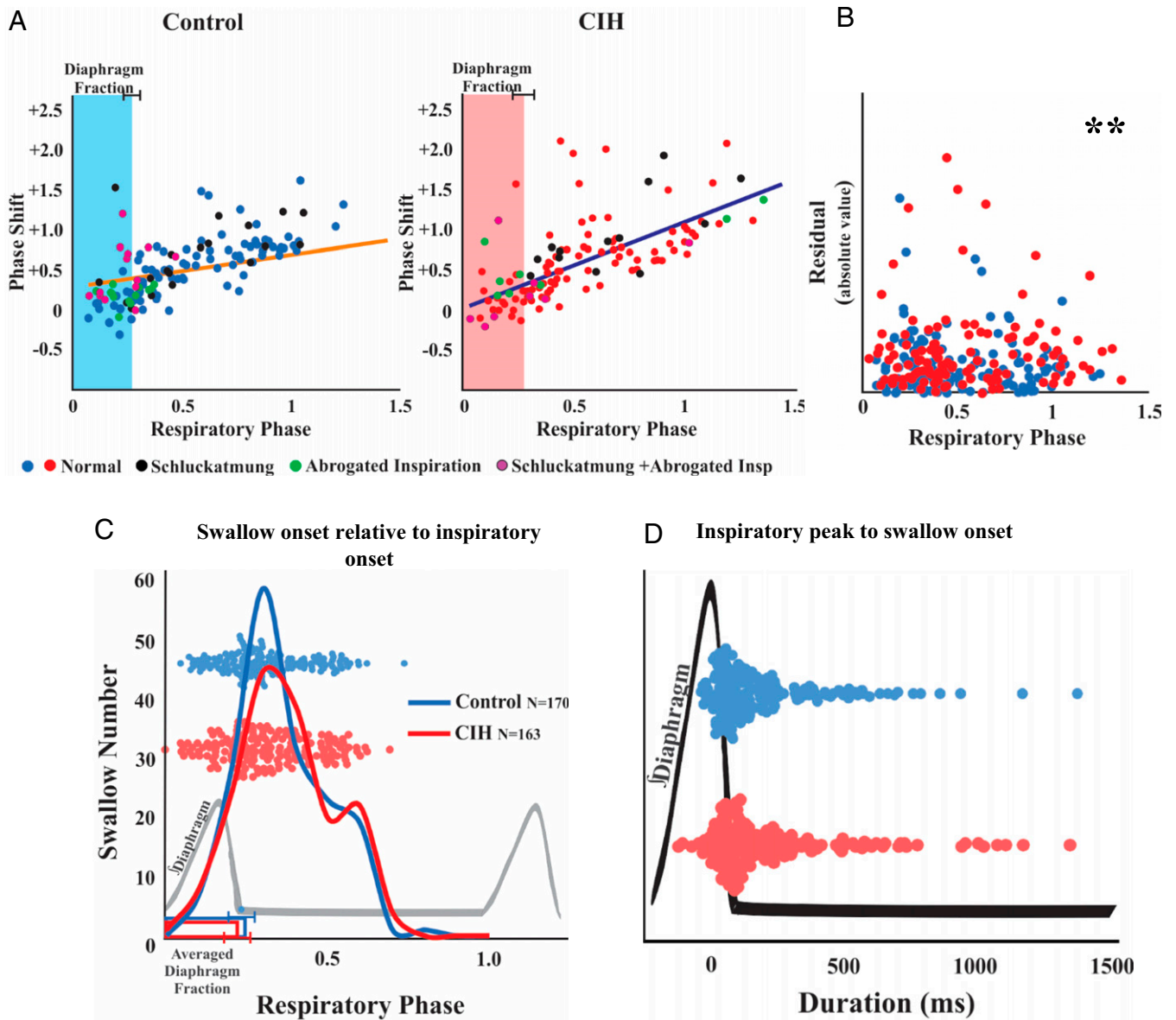
Fig. 5. Swallowing–breathing coordination becomes unpredictable after CIH exposure. (*A*) Swallow-related respiratory resetting curves for control and CIH conditions. Calculations for each axis are depicted in Fig. 6*D*. The red and blue dots represent normal swallows in control and CIH, respectively. The black dots represent schluckatmung activity, green represents the abrogated inspiratory burst, and purple represents the multimodal diaphragm activity. The orange line is the line of best fit for control, and blue is the line of best fit for the CIH graph. (*B*) Residual plot showing absolute values of distances from the line of best fit. A test of differences of the residuals shows CIH is significantly more variable than control (mean ± SD, $P = 0.007$, $n = 40$ and 37, respectively). (*C*) Histogram of swallowing in relation to the onset of inspiration, showing more occurrences of swallowing during inspiration in CIH-exposed mice. (*D*) Dot plot of each swallow in relation to the inspiratory peak. The majority of swallows occur during postinspiration, and more incidences of swallowing during inspiration when exposed to CIH. Each dot represents one swallow.

does not induce changes to the respiratory rhythm; rather, it is the timing of swallowing during the respiratory cycle that depicts when the next inspiratory burst is advanced or delayed.

We saw an increased prevalence of swallows in CIH-exposed animals occurring during the inspiratory phase. Fig. 5*C* shows a histogram of the swallowing–breathing phase relationship. Swallow activity aligned to the onset of inspiration reveals no difference in the coordination of swallowing and breathing between control and CIH conditions. Swallows aligned in relation to the peak of inspiratory activity, as defined by the peak diaphragmatic activity, allowed for better separation of swallows occurring during the different phases of breathing: inspiration (onset of the diaphragm to the peak), postinspiration (peak diaphragm to the offset), and expiration (offset of the diaphragm to the onset of the next diaphragm burst) (Fig. 5*D*).

Exposure to CIH Blunts preBötC Excitatory Modulatory Effects.

Stimulating Dbx1 neurons in the preBötC. All examined animals ($n = 9$) responded to water stimulation with swallows before and during *Dbx1* stimulation, and we observed no change in the number of water-evoked swallows. There was also no change in the oropharyngeal sequence as seen during control conditions. However, the onset of swallows was significantly delayed (from 274 ± 161 to 555 ± 358 ms, $P = 0.02$), resulting in swallows occurring during later stages of expiration (Fig. 7*A*). In CIH-exposed animals, 30% of swallows were characterized with schluckatmung during baseline and 33% were characterized with schluckatmung during excitatory preBötC stimulation.

Inhibiting Dbx1 neurons in the preBötC. We found no changes in swallow-related or swallowing–breathing-related parameters
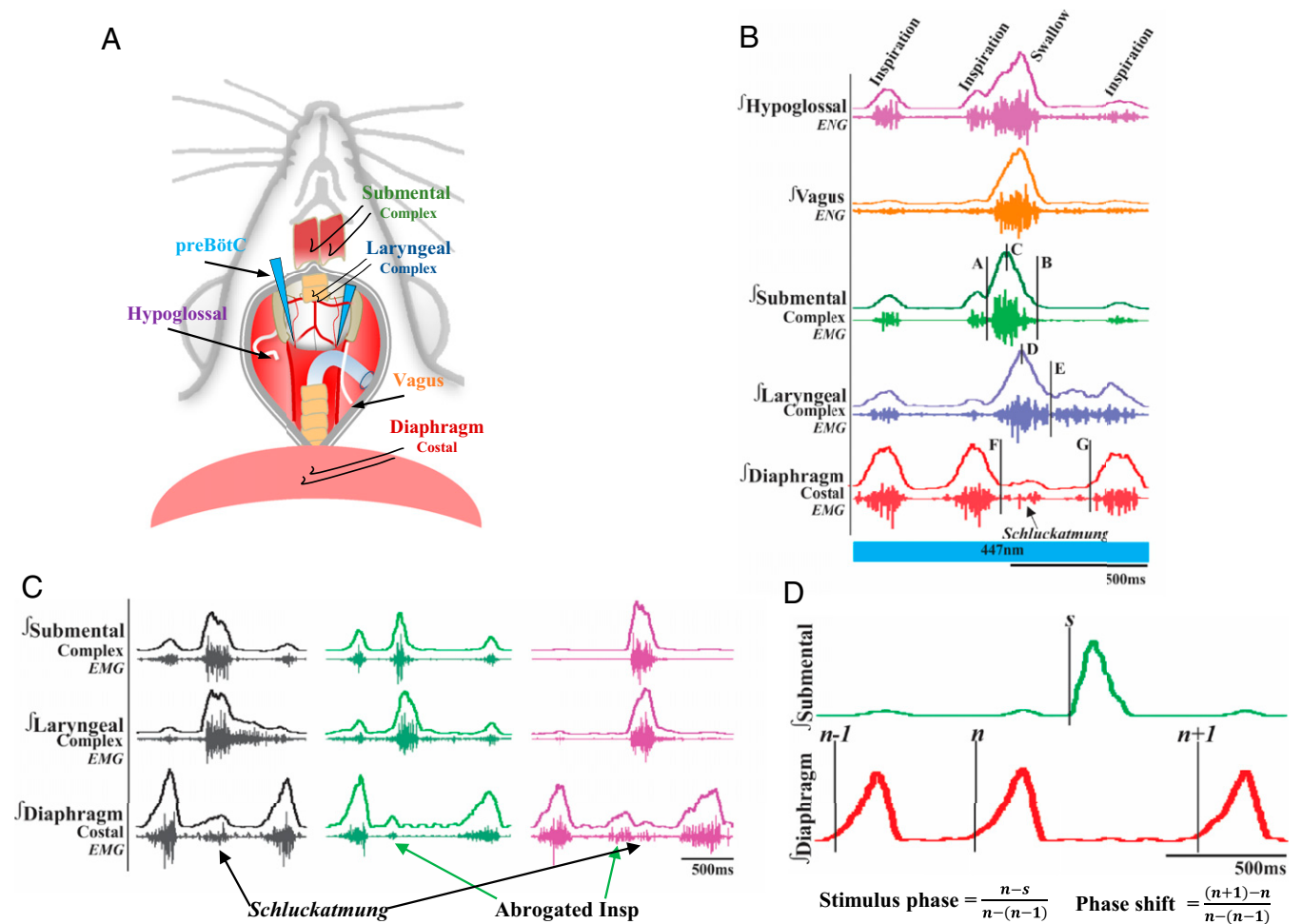
Fig. 6. (*A*) Schematic of the in vivo preparation, including all nerves and muscles recorded from and optrode placement. (*B*) Representative EMG traces of a water-induced swallow in a CIH-exposed animal. The blue bar represents simultaneous water swallow and optogenetic stimulation. Swallow duration (B-A), swallow sequence (D-C), diaphragm interburst interval (G-F), and inspiratory delay duration (G-E) are shown. (*C*) Representative traces of water-induced atypical swallows. The black shows diaphragm activity during a swallow termed schluckatmung. The green shows swallow-related inspiratory burst suppression known as an abrogated inspiration. Purple shows a swallow with both an abrogated inspiratory burst and a schluckatmung, displaying the multimodal functions of the diaphragm. Marckwald (81) described this in the rabbit, stating that when a swallow occurs at the end of inspiration, the movement is divided. The black and green traces are from recordings under CIH conditions, and the purple trace is from recordings in control conditions. (*D*) Representative traces depicting how the stimulus phase and phase shift are calculated for the phase-shift plots in Fig. 5. This example was taken from a recording under control conditions.

when *Dbx1* was inhibited in CIH-exposed mice (*n* = 5). In CIH-exposed animals, 4% of swallows were characterized with schluckatmung during baseline and 5% were characterized with schluckatmung during excitatory preBötC inhibition.

Stimulating Vglut2 neurons in the preBötC. In CIH-exposed animals (*n* = 8), the integrated X amplitude significantly increased during *Vglut2* stimulation (from 78 ± 14 to 93 ± 16% of maximum, *P* = 0.03) (Fig. 7*B*). In CIH-exposed animals, swallow number significantly decreased during *Vglut2* stimulation (from 5 ± 3 to 3 ± 1, *P* = 0.03).

Stimulating Sst neurons in the preBötC. Unlike what was shown in control conditions, we saw no change in swallow onset when *Sst* neurons were stimulated in CIH-exposed mice. We found a significant increase in the diaphragm interburst interval duration (from 625 ± 180 to 791 ± 196 ms, *P* = 0.03) and inspiratory delay (from 249 ± 152 to 336 ± 112 ms, *P* = 0.03) during stimulation of *Sst* neurons within the preBötC (*n* = 8) (Fig. 7*C*). There was no change in swallow number and only one occurrence of schluckatmung during stimulation.

Stimulating Vgat neurons in the preBötC. We found a significant increase in the interburst interval duration (from 691 ± 199 to 1,576 ± 795 ms, *P* = 0.03) and inspiratory delay (from 301 ± 205 to 737 ± 407 ms, *P* = 0.02) during stimulation of *Vgat* neurons within the preBötC when exposed to CIH (*n* = 7) (Fig. 7*D*). The number of swallows significantly decreased during *Vgat* stimulation (from 5 ± 2 to 3 ± 1, *P* = 0.002).

Sex Differences.
Genetic cohorts combined. In control animals, swallows in males occur significantly later in expiration than they did in females (238 ± 127 versus 127 ± 92 ms, *P* = 0.004). In control conditions, male mice weighed significantly more than female mice (28 ± 3 versus 21 ± 2 g, *P* = 0.0001). In mice exposed to CIH, males weighed significantly more than females (22 ± 3 versus 18 ± 1 g, *P* = 0.0001). *SI Appendix*, Tables S4–S9 shows descriptive statistics of all swallow-related sex-specific parameters.
Vgat stimulation. There are no swallow-related sex-specific differences in the control or CIH-exposed animals during baseline or preBötC stimulation.
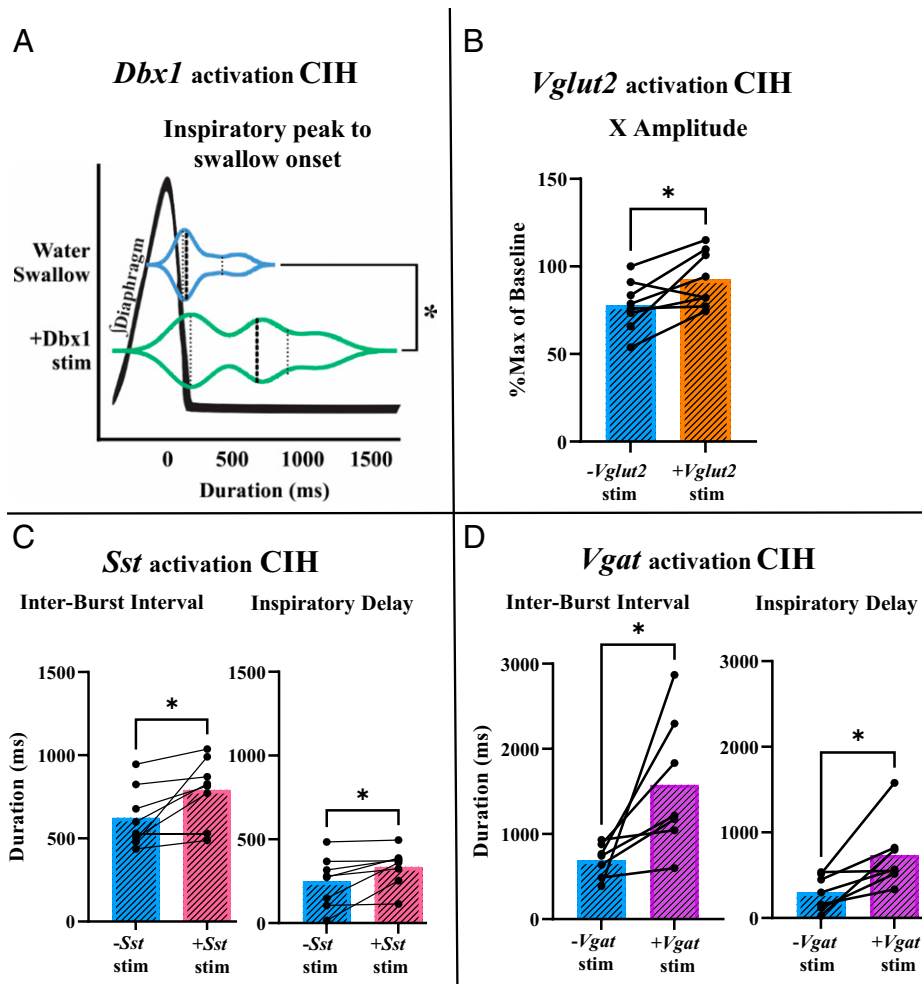
Fig. 7. Effects of CIH on swallowing–breathing coordination during preBötC stimulation. (*A*) Violin plot showing the shift in swallowing–breathing coordination during *Dbx1* stimulation (green). The dark dotted line depicts the average time a swallow occurs in relation to peak diaphragm activity (mean ± SD, $P = 0.02$, $n = 9$). (*B*) Swallow-related vagal amplitude increased during *Vglut2* stimulation when exposed to CIH (mean ± SD, $P = 0.03$, $n = 8$). (*C* and *D*) Diaphragm interburst interval and inspiratory delay significantly increased during (*C*) *Sst* stimulation (mean ± SD, $P = 0.03$ (interburst interval), $P = 0.03$ (inspiratory delay, $n = 8$) and (*D*) *Vgat* stimulation (mean ± SD, $P = 0.03$, $P = 0.02$, $n = 7$) when exposed to CIH.

Vglut2 stimulation. There are no swallow-related sex-specific differences during baseline control conditions. During *Vglut2* stimulation, females have a significantly longer laryngeal delay in the swallow sequence than males (50 ± 17 versus 1 ± 30 ms, $P = 0.02$).

CIH-exposed males have a significantly longer interburst interval ($1{,}394 \pm 615$ versus 592 ± 198 ms, $P = 0.05$) and inspiratory delay (857 ± 538 versus 193 ± 59 ms, $P = 0.05$) during baseline swallows. During *Vglut2* stimulation in CIH-exposed animals, there are no observed swallow-related sex-specific differences.

Dbx1 activation. In control males, swallows in occur significantly later in expiration (278 ± 92 versus 75 ± 55 ms, $P = 0.01$) compared to females. Swallows occurring during *Dbx1* stimulation show no sex-specific differences. This is most likely because two of the male animals did not swallow during *Dbx1* stimulation, making the comparison between two male and five females.

Compared with females, males exposed to CIH have a significant longer swallow-related XII duration (406 ± 113 versus 251 ± 58 ms, $P = 0.05$), as well as a significantly longer delay in swallow-related laryngeal closure without (124 ± 40 versus 66 ± 20 ms, $P = 0.02$) and with (107 ± 49 versus 23 ± 50 ms, $P = 0.04$) *Dbx1* stimulation.

Dbx1 inhibition. There are no swallow-related sex-specific differences in the control or CIH-exposed animals during baseline or preBötC stimulation.

Sst activation. We saw no swallow-related sex-specific differences in control animals during baseline or preBötC stimulation. CIH-exposed males have a significantly longer interburst interval (908 ± 100 versus 597 ± 153 ms, $P = 0.01$) and inspiratory delay (399 ± 55 versus 231 ± 107 ms, $P = 0.02$) in swallows stimulated under *Sst* activation.

Discussion

Understanding how breathing is coordinated and integrated with other behaviors is of fundamental importance. This is particularly important for swallowing, which shares many of the same anatomical structures as breathing. To avoid aspiration, swallowing should not coincide with inspiration. Indeed, here we find that water swallows can prematurely inhibit ongoing inspiratory activity, which was reflected in abrogated inspiratory diaphragmatic activity. While it is thought that the preBötC prevents concurrent inspiration and swallowing by inhibiting the swallow pattern generator (52), it is a bit more complex due to the multimodal function of the diaphragm.

The concept that different phases of breathing are generated by distinct excitatory networks (53) suggests mutually inhibitory interactions between the networks controlling inspiration and swallowing. The network generating inspiratory activity, the preBötC, is well described, and the neurons critical for inspiratory rhythmogenesis, the *Dbx1* neurons, as well as inhibitory and other glutamatergic neurons within the preBötC, are amenable to optogenetic manipulations using transgenic mouse lines (54). Stimulating inhibitory preBötC (*Vgat*) neurons delayed the onset of the next respiratory cycle but did not interfere with swallowing (Fig. 8*A*). This result suggests that the inhibition of swallowing during inspiration is not produced by the inhibitory neurons within the preBötC. In this context, these inhibitory preBötC neurons only regulate breathing. Instead, we find that activating *Dbx1* neurons decreases the propensity to swallow, which occurred concurrently with an increased drive for breathing. Thus, the decreased propensity to swallow could be a consequence of the *Dbx1*-induced increased drive for breathing rather than a swallow-specific inhibition by the *Dbx1* neurons. However, our data also indicate that stimulating *Dbx1* neurons alters upper airway coordination critical for swallowing. *Dbx1* activation specifically delayed the peak activation of the laryngeal complex following the activation of the submental complex (Fig. 8*A*). This delay poses a risk for aspiration, because a delay in closure of the vocal folds while food passes through the pharynx leaves opportunity for food to penetrate into the larynx and then potentially to the lungs. However, inhibition of *Dbx1* neurons did not cause an alteration in swallow sequence; rather, it caused an increase in laryngeal closure duration, supporting our proposal the *Dbx1* neurons in the preBötC have connections to the swallow pattern generator. Inhibition of Dbx1 neurons also delayed the onset of the next respiratory cycle, congruent with reports indicating a decrease in respiratory frequency (55). Broad stimulation of excitatory *Vglut2* neurons in the preBötC increased swallow-related nerve amplitude (Fig. 8*A*). This was not seen during *Dbx1* stimulation, which indicates the excitatory feedback from preBötC to swallow pattern generators is *Dbx1* specific. Stimulation of excitatory *Sst* neurons at the preBötC pushed swallow occurrence to later into the respiratory cycle, suggesting indirect, inhibitory connections from the preBötC to the putative swallow pattern generator (Fig. 8*A*). Though somatostatin neurons are a subset of excitatory neurons within the preBötC, our findings suggest they act as an inhibitory neuromodulator, which is consistent with their reported role in breathing (34, 35).

Interestingly, the disturbance of the swallow sequence caused by stimulating *Dbx1* neurons was similarly caused by CIH (Fig. 8*B*). Thus, the generation of swallowing following CIH exposure has characteristics that are reminiscent of those evoked by activating the inspiratory network. Moreover, this sequential interference of swallowing by the inspiratory network is not present when stimulating and inhibiting *Dbx1* neurons following CIH exposure. In addition, the increased drive for breathing ceased to depress swallow drive during *Dbx1* stimulation in CIH-exposed mice and pushed swallows to occur during the later stages of expiration. This finding indicates that CIH interferes with the phase-dependent interactions between the respiratory and the swallowing networks.

CIH-induced abnormalities were observed not only for the respiratory effects on swallowing but also with regards to the reciprocal influence from swallowing onto the respiratory network. Here we show that swallowing resets ongoing inspiratory rhythmogenesis. The later a swallow occurs in the respiratory cycle, the bigger the delay of the subsequent inspiratory cycle. This inspiratory reset was significantly more variable following exposure to CIH. Swallowing often caused long delays in the onset of the next inspiratory cycle. Indeed, following CIH exposure, respiratory rhythmogenesis was severely inhibited by swallows during preBötC activation and did not resume for a prolonged time period, which was reflected in long-lasting swallow-related interburst intervals of the diaphragm.

The mechanisms in which the swallow pattern generator and respiratory pattern generator are coordinated with breathing to ensure a patent airway have yet to be fully determined. It is thought that the presumed swallow center in the NTS projects to pharyngeal and laryngeal motoneurons in the NA. Thus, inhibition of breathing during the pharyngeal phase of swallowing could involve direct projection from the NTS to respiratory centers such as preBötC (45). This connection could also simultaneously stimulate pharyngeal contraction and laryngeal
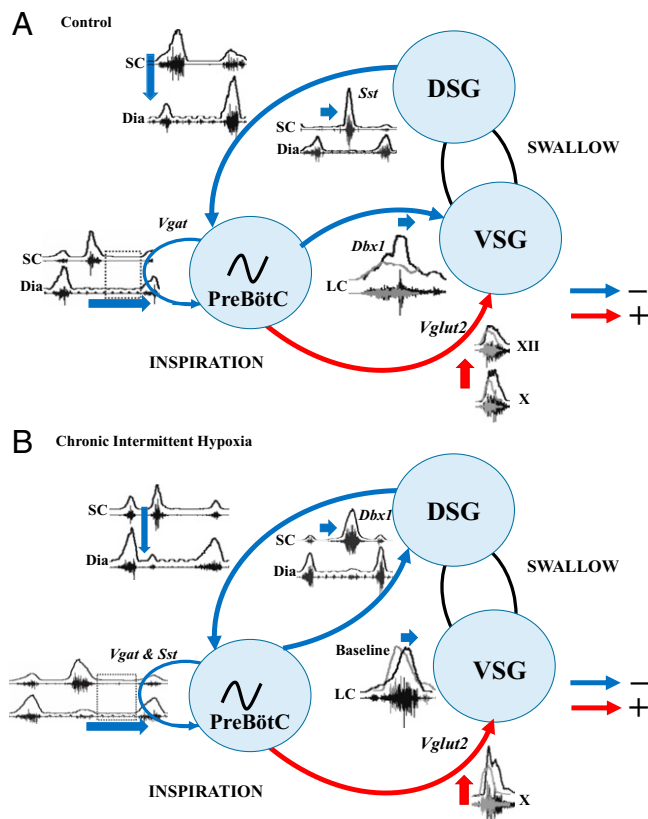

Fig. 8. Proposed mechanisms of swallowing–breathing coordination between inspiratory and swallow centers. (*A*) Under control conditions, we suggest inhibitory (blue) connections between the DSG and the preBötC due to a swallow (submental complex, SC) inhibiting the inspiratory burst (diaphragm, Dia). Stimulation of *Dbx1* neurons delays the laryngeal complex (LC) during swallowing, and stimulation of *Sst* neurons pushes swallow occurrence later into the respiratory cycle, suggesting inhibitory connections from the preBötC to the putative swallow pattern generators. Inhibition of *Dbx1* neurons disinhibits swallow pattern generators increasing, laryngeal closure duration. An increase in swallow-related hypoglossal (XII) and vagus (X) nerve amplitude during *Vglut2* stimulation suggests excitatory (red) connections from the preBötC and VSG. Stimulation of *Vgat* neurons increases diaphragm interburst interval, as well as inhibition of *Dbx1* neurons, suppressing the incoming inspiratory burst and suggesting inhibitory feedback from the preBötC onto itself, not involving swallow centers. (*B*) The same mechanisms were present when the mice were exposed to CIH except for *Dbx1* stimulation, which mimicked control *Sst* stimulation, and *Sst* stimulation, which mimicked *Vgat* stimulation. Instead, water swallows without any preBötC stimulation had the same response as *Dbx1* stimulation in control conditions. We propose CIH modulates the *Dbx1* neurons and destabilizes the preBötC, delaying the laryngeal complex during swallowing and mimicking what is seen during optogenetic stimulation of *Dbx1* neurons.

closure (45). The current study suggests neurons from the preBötC connect to the laryngeal motoneurons of the NA (56), resulting in delayed laryngeal closure during *Dbx1* stimulation and increased laryngeal closure duration during *Dbx1* inhibition and *Vglut2* stimulation.

However, our experiments did not directly test the influence of the swallowing network on the respiratory network, given that the critical neurons responsible for swallowing have not been identified. Future studies aimed at unraveling interactions between the NTS and the ventral components of the putative swallow pattern generator will be important, but such studies depend on the identification of the neurons critical for swallowing. Future studies also need to address the role of these swallow-related neurons in alert mice as opposed to the anesthetized prep.

Our findings are consistent with disordered swallowing, which is caused by lesions in the brainstem (57). Lesions in the dorsal pons, specifically the Kolliker-Fuse nucleus, decrease swallow dominance over breathing (58). Thus, we want to emphasize that swallowing–breathing coordination is not entirely controlled by the medulla and that rostral structures along the neural axis also play important roles (59). It is also known that respiratory-related neurons are activated and inhibited during both breathing and swallowing (60). The medullary intermediate reticular formation within the ventral respiratory group is thought to be a multimodal integration hub that contains neurons active during both swallowing and breathing, receives afferent information, and distributes this information to various motoneurons pools (61). The respiratory rhythm is reset as the drive for swallowing is increased (62). There is evidence that preinspiratory neurons within the preBötC have concurrent activation during swallowing (63), which suggests a role of the preBötC in swallowing–breathing coordination. It is pertinent for the swallow neural network to supersede the breathing network drive and reconfigure the respiratory motor pattern to 1) inhibit inspiration, which in turn inhibits inspiratory-related muscles; 2) activate postinspiration via closure of the glottis to ensure a patent airway; and 3) activate expiration for continuation of a patent airway, creating a swallowing–breathing apnea, for the reset of the incoming inspiration. The reorganization of respiratory-related networks produces changes in motor pattern to move the bolus through the pharynx and into the esophagus (64).

Discoordination of swallowing and breathing leads to significant clinical disorders. A large portion of the OSA and COPD patient population exhibits signs of impaired swallow function (65–68). Oropharyngeal dysphagia is an underdiagnosed comorbidity of OSA (69, 70), and this study looks at the physiological mechanisms of OSA and provides a mouse model that mimics many of the dysphagic outcomes seen clinically after CIH exposure. Typical dysphagic characteristics in OSA patients include longer latency of swallow reflex and decreased inspiratory suppression time (50, 51, 68) occurring slightly earlier in the expiratory phase (71), premature oral leakage (72), and increased laryngeal excursion time and swallow-related apnea, or swallow-related expiratory duration (68, 73). This study teased apart many aspects of central swallowing–breathing coordination, a mechanism thought to be associated with OSA-related dysphagia (73). We reported that manipulation of various neurons types in the preBötC mimic multiple dysphagic characteristics in OSA, suggesting the importance of a normal functioning medullary respiratory center. The severity of OSA and community-acquired pneumonia are directly related, with OSA almost tripling the risk of pneumonia (74), and dysphagia contributing to this increased risk pneumonia. However, the severity of OSA and dysphagia is not correlated, though an increase in the prevalence of dysphagia was seen in females (68, 72). With a growing population of dysphagia in OSA, there is limited knowledge and training in OSA for clinicians such as speech-language pathologists (75). Continuing research on the effect of CIH on the neural circuitry and how swallowing–breathing coordination is affected will be critical to further the clinical understanding of this growing patient population.

Methods

Animals. Adult (postnatal day P53 to P131, average P79) male and female mice were bred at the Seattle Children's Research Institute (SCRI) and used for all experiments. *Vglut2-ires-cre*, *Vgat-ires-cre*, and *Sst-ires-cre* homozygous breeder lines were obtained from The Jackson Laboratory (stock 028863, 016962, and 013044, respectively). Heterozygous *Dbx1creERT2* mice were donated by Del Negro (College of William and Mary, Williamsburg, VA), originally created by Josh Corbin [George Washington School of Medicine and Health Sciences, Washington, DC (76)], and a homozygous breeder line was generated at SCRI. Cre mice were crossed with homozygous mice containing a floxed STOP channelrhodopsin fused to an enhanced yellow fluorescent protein (Ai32) reporter sequence from The Jackson Laboratory (stock 024109). The homozygous *Dbx1creERT2* were also crossed with homozygous mice containing a floxed STOP archaerhodopsin fused to an enhanced freen fluorescent protein (Ai40D) reporter sequence from The Jackson Laboratory (stock 021188). All mouse lines are routinely genotyped for confirmation of their homozygous gene type. Mice were randomly selected from the resulting litters by the investigators. *Dbx1creERT2* dams were plug checked and injected at embryonic day E10.5 with tamoxifen [24 mg/kg intraperitoneally (i.p.)] to target preBötC neurons (36, 37). Offspring were group housed with ad libitum access to food and water in a temperature-controlled (22 $\pm$ 1 °C) facility with a 12:12 h light:dark cycle. All experiments and animal procedures were approved by SCRI's animal care and use committee and were conducted in accordance with NIH guidelines (77).

CIH. Mice of the *Vglut2*cre, *Dbx1*cre, *Sst*cre, and *Vgat*cre varying optogenetic lines were kept in collective cages with food and water ad libitum placed inside custom-built chambers (volume: 185 L) equipped with gas injectors, as well as oxygen (O_2) sensors (Oxycycler, Huff Technologies Inc.). One chamber was used for CIH, and the other was used for control. The CIH group was exposed to intermittent episodes of hypoxia: continuous injection of nitrogen (N_2) for 60 s, in order to reduce the percentage of inspired O_2 inside the chamber from 21% to a range of 4.5 to 5%, and then continuous injection of compressed air for 5 min into the chamber to return the percentage of O_2 to 21% before the start of a new hypoxia cycle. Compressed air and N_2 injection into the chambers was regulated by a valve system, automatically operated by customized software (Oxycycler, Huff Technologies Inc.). This protocol was repeated with 80 bouts per day (8 h) during the light cycle in a 12:12 h light:dark cycle room, for an average of 21 d. Of note, the range was 11 to 29 days, but internal analysis of a pilot 10-d protocol showed no difference from the 21-d protocol and these were combined in this study. In the remaining 16 h, the mice were kept under normoxic conditions (21% O_2). Control mice were kept in a replicated chamber under normoxic conditions (21% O_2), 24 h/d, during the same period as the CIH protocol.

In Vivo Experiments. The same experimental protocol was performed for all control and CIH *Vglut2*cre, *Dbx1*cre, *Sst*cre, and *Vgat*cre Ai32 mice. At the end of the CIH or control protocol, adult mice were initially anesthetized with 100% O_2 and 1.5% isoflurane (Aspen Veterinary Resources Ltd, Liberty, MO) for 2 to 3 min in an induction chamber. Once the breathing slowed, they were injected with urethane (1.5 mg.kg i.p., Sigma-Aldrich, St. Louis, MO) and placed supine on a custom surgical table. The trachea was exposed through a midline incision and cannulated caudal to the larynx with a curved (180°) tracheal tube (polytetrafluoroethylene 24G, Component Supply, Sparta, TN). Mice were then allowed to spontaneously breathe 100% O_2 for the remainder of the surgery and experimental protocol. Fig. 6*A* shows placement of bipolar electromyogram (EMG) electrodes in the costal diaphragm to monitor respiratory rate and heart rate throughout the experiment. Core temperature was maintained through a water heating system (PolyScience, Niles, IL) built into the surgical table. Adequate

depth of anesthesia was determined via heart and breathing rate, as well as lack of toe pinch response every 15 min. The hypoglossal (XII) and vagus (X) nerves were then dissected, followed by cannulation of the trachea. The recurrent laryngeal nerve was carefully dissected away from each side of the trachea before the cannula was tied in and sealed with superglue to ensure no damage to the recurrent laryngeal nerve. The trachea and esophagus was then cut to detach at the rostral end just caudal to the cricoid cartilage, preserving the arytenoids and bilateral recurrent laryngeal nerves. A tube filled with compressed air was attached to the cannulated trachea to provide supplemental O_2 throughout the experiment. The occipital bone was removed, followed by continuous perfusion of the ventral medullary surface with warmed ($\sim$36 °C) artificial cerebral spinal fluid (aCSF: 118 mM NaCl, 3 mM KCl, 25 mM $NaHCO_3$, 1 mM NaH_2PO_4, 1 mM $MgCl_2$, 1.5 mM $CaCl_2$, and 30 mM D-glucose) equilibrated with carbogen (95% O_2 and 5% CO_2) by a peristaltic pump (Dynamax RP-1, Rainin Instrument Co., Emeryville, CA). The XII and X nerves were isolated unilaterally, cut distally, and recorded from using a fire-polished pulled borosilicate glass (B150-86-15, Sutter Instrument, Novato, CA) filled with aCSF connected to the monopolar suction electrode (A-M Systems, Sequim, WA) and held in a three-dimensional micromanipulator (Narishige, Tokyo, Japan). Multiple bipolar EMGs using 0.002- and 0.003-inch coated stainless steel wires (parts 790600 and 79100, respectively, A-M Systems), according to the techniques of Basmajian and Stecko (78), simultaneously recorded activity from several swallow- and respiratory-related muscle sites and were placed using 30G hypodermic needles (part 305106, BD Precision Glide, Franklin Lakes, NJ) in the 1) submental complex, which consists of the geniohyoid, mylohyoid, and digastric muscles, to determine swallow activity; 2) the laryngeal complex, consisting of the arytenoid muscles (transverse, oblique, thyroarytenoid, and posterior cricoarytenoid muscles), to determine laryngeal closure during swallows, as well as postinspiratory activity; and 3) the costal diaphragm, used to measure the multifunctional activity for inspiration; abrogated inspiration, a decrease in diaphragm duration and amplitude due to swallow activity; and schluckatmung, a less common diaphragmatic activation during swallow activity (Fig. 6C). Glass fiber optic (200 μm diameter) connected to a blue (447 nm) laser and diode pumped solid-state driver (Opto Engine LLC, Salt Lake City, UT) or lime (565 nm) laser and light-emitting diode driver (Thorlabs) was placed bilaterally in light contact with the brainstem over the top of the predetermined preBötC (26) (Fig. 6A).

Stimulation Protocols. First, swallowing was stimulated by injecting 0.1 cmL of water into the mouth using a 1.0-cmL syringe connected to a polyethylene tube. Second, 10 s of continuous transistor-transistor-logic laser stimulation at preBötC while simultaneously injecting 0.1 cmL of water into the mouth triggered a swallow during preBötC activation (Fig. 6B). The lasers were each set to 0.75 mW when using the 447-nm wavelength and to 3.0 mW when using the 565-nm wavelength and triggered using Spike2 software (Cambridge Electronic Design, Cambridge, UK). These stimulation protocols were performed in all control and CIH *Vglut2*cre, *Dbx1*cre, *Sst*cre, and *Vgat*cre Ai32 and Ai40D mice. Changes in neural activity via optogenetic stimulation were confirmed with intracellular recordings from slices (26).

Analysis. All electroneurogram (ENG) and EMG activity was amplified and band-pass filtered (0.03 to 1 kHz) by a differential alternating current amplifier (model 1700, A-M Systems), acquired in an analog to digital converter (CED 1401, Cambridge Electronic Design), and then integrated, rectified, smoothed, and stored using Spike2 software (Cambridge Electronic Design).

Fig. 6B shows swallow duration (B-A) determined by the onset to the termination of the submental complex. If the submental complex muscles were not available, then it was determined by the onset to the offset of the XII. Swallow sequence (D-C) was calculated as the time difference between the peak of the laryngeal and that of the submental complex. Traditionally, swallow sequence is calculated as the difference in laryngeal and submental onset, though we found in the mouse this delay is consistent in the peak activation. Swallow-related diaphragm interburst interval (G-F) was calculated as the offset of the diaphragm to the onset of the proceeding breath. Inspiratory delay (G-E) was defined as the offset of the swallow-related laryngeal activity to the onset of the preceding breath. Schluckatmung duration was determined by the onset to the offset of the diaphragm during a swallow. Duration of each nerve and muscle was determined by the onset to the offset of that respective nerve/muscle during a swallow. Swallow amplitude was calculated as the percentage of the maximum amplitude during baseline trial (no laser stimulation) conditions for each nerve and muscle during swallow activity. Fig. 6D depicts respiratory phase reset curves calculated by defining the respiratory cycle as the onset of the diaphragm to the onset of the subsequent diaphragm activity. The phase shift elicited by each stimulation of water was calculated as the duration of the respiratory cycle containing the stimulus divided by the preceding respiratory cycle. The phase of swallow stimulation (respiratory phase) was calculated as the time between the onset of the inspiration (diaphragm) and the stimulus onset divided by the expected phase. The average phase shift was then plotted against the respiratory phase in bins containing one-tenth of the expected phase (26). Swallow histogram plots were created by the phase of breathing in which swallowing occurred, calculated as the onset of inspiration to the onset of swallow divided by the respiratory cycle duration and plotted against the number of swallows that occurred within the one-tenth binned respiratory phase (Fig. 5C). Swallowing was also plotted in relation to the peak activation of the diaphragm as a duration, with zero equaling the peak of the inspiratory-related diaphragm activity (Fig. 5D). These parameters were analyzed in both control and CIH animals, as well as before and during preBötC laser stimulation.

All data are expressed as mean $\pm$ SD. Statistical analyses were performed using GraphPad Prism 6 (GraphPad Software, Inc.). For comparisons between control and CIH, males and females, a two-tailed Student's t test was used for unpaired data. Comparison between baseline and stimulus within the same group was made by a paired Student's t test. Differences were considered significant at $P \leq 0.05$. Investigators were not blinded during analysis. Sample sizes were chosen on the basis of previous studies.

Data Availability. Data related to this work are available in Figshare (79). All other study data are included in the article and/or *SI Appendix*.

1. K. Hartmann, M. Brecht, A functionally and anatomically bipartite vocal pattern generator in the rat brain stem. *iScience* **23**, 101804 (2020).
2. J. D. Hoffmeister, C. L. Ulmschneider, C. A. Jones, M. R. Ciucci, T. M. McCulloch, Measurement of pharyngeal air pressure during phonation using high-resolution manometry. *J. Speech Lang. Hear. Res.* **64**, 3456–3464 (2021).
3. G. Holstege, H. H. Subramanian, Two different motor systems are needed to generate human speech. *J. Comp. Neurol.* **524**, 1558–1577 (2016).
4. Z. Kotmanova et al., GABA-ergic neurotransmission in the nucleus of the solitary tract modulates cough in the cat. *Respir. Physiol. Neurobiol.* **257**, 100–106 (2018).
5. K. A. R. Rose et al., Scaling of axial muscle architecture in juvenile Alligator mississippiensis reveals an enhanced performance capacity of accessory breathing mechanisms. *J. Anat.* **239**, 1273–1286 (2021).
6. D. P. Attenburrow, V. A. Goss, The mechanical coupling of lung ventilation to locomotion in the horse. *Med. Eng. Phys.* **16**, 188–192 (1994).
7. T. Waselius, J. Wikgren, M. Penttonen, M. S. Nokia, Breathe out and learn: Expiration-contingent stimulus presentation facilitates associative learning in trace eyeblink conditioning. *Psychophysiology* **56**, e13387 (2019).
8. T. Waselius, J. Wikgren, H. Halkola, M. Penttonen, M. S. Nokia, Learning by heart: Cardiac cycle reveals an effective time window for learning. *J. Neurophysiol.* **120**, 830–838 (2018).
9. M. Hammer, C. Schwale, J. Brankačk, A. Draguhn, A. B. L. Tort, Theta-gamma coupling during REM sleep depends on breathing rate. *Sleep (Basel)* **44**, zsab189 (2021).
10. A. B. L. Tort, M. Hammer, J. Zhang, J. Brankačk, A. Draguhn, Temporal relations between cortical network oscillations and breathing frequency during REM sleep. *J. Neurosci.* **41**, 5229–5242 (2021).
11. J. F. Bosma, S. G. Fletcher, The upper pharynx. A review. II. Physiology. *Ann. Otol. Rhinol. Laryngol.* **71**, 134–157 (1962).
12. A. J. Miller, Deglutition. *Physiol. Rev.* **62**, 129–184 (1982).
13. V. Negus, *The Mechanism of Swallowing* (SAGE Publications, 1942).
14. S. M. Barlow, Central pattern generation involved in oral and respiratory control for feeding in the term infant. *Curr. Opin. Otolaryngol. Head Neck Surg.* **17**, 187–193 (2009).
15. K. Matsuo, J. B. Palmer, Anatomy and physiology of feeding and swallowing: Normal and abnormal. *Phys. Med. Rehabil. Clin. N. Am.* **19**, 691–707, vii (2008).
16. R. W. Doty, J. F. Bosma, An electromyographic analysis of reflex deglutition. *J. Neurophysiol.* **19**, 44–60 (1956).
17. A. J. Thexton, A. W. Crompton, R. Z. German, Electromyographic activity during the reflex pharyngeal swallow in the pig: Doty and Bosma (1956) revisited. *J Appl Physiol (1985)* **102**, 587–600 (2007).

18. A.-W. Heemskerk, R. A. C. Roos, Aspiration pneumonia and death in Huntington's disease. *PLoS Curr.* **4**, RRN1293 (2012).
19. K. Nakashima *et al.*; Tottori University Parkinson's Disease Epidemiology (TUPDE) Study Group, Prognosis of Parkinson's disease in Japan. *Eur. Neurol.* **38** (suppl. 2), 60–63 (1997).
20. C. M. Beard *et al.*, Cause of death in Alzheimer's disease. *Ann. Epidemiol.* **6**, 195–200 (1996).
21. S. Todd, S. Barr, A. P. Passmore, Cause of death in Alzheimer's disease: A cohort study. *QJM* **106**, 747–753 (2013).
22. C. Gestreau, S. Milano, A. L. Bianchi, L. Grélot, Activity of dorsal respiratory group inspiratory neurons during laryngeal-induced fictive coughing and swallowing in decerebrate cats. *Exp. Brain Res.* **108**, 247–256 (1996).
23. T. E. Dick, Y. Oku, J. R. Romaniuk, N. S. Cherniack, Interaction between central pattern generators for breathing and swallowing in the cat. *J. Physiol.* **465**, 715–730 (1993).
24. J. C. Smith, H. H. Ellenberger, K. Ballanyi, D. W. Richter, J. L. Feldman, Pre-Bötzinger complex: A brainstem region that may generate respiratory rhythm in mammals. *Science* **254**, 726–729 (1991).
25. S. Ashhad, J. L. Feldman, Emergent elements of inspiratory rhythmogenesis: Network synchronization and synchrony propagation. *Neuron* **106**, 482–497.e4 (2020).
26. N. A. Baertsch, H. C. Baertsch, J. M. Ramirez, The interdependence of excitation and inhibition for the control of dynamic breathing rhythms. *Nat. Commun.* **9**, 843 (2018).
27. J.-M. Ramirez, N. A. Baertsch, The dynamic basis of respiratory rhythm generation: One breath at a time. *Annu. Rev. Neurosci.* **41**, 475–499 (2018).
28. W. Tan *et al.*, Silencing preBötzinger complex somatostatin-expressing neurons induces persistent apnea in awake rat. *Nat. Neurosci.* **11**, 538–540 (2008).
29. K. Kam, J. W. Worrell, W. A. Janczewski, Y. Cui, J. L. Feldman, Distinct inspiratory rhythm and pattern generating mechanisms in the preBötzinger complex. *J. Neurosci.* **33**, 9235–9245 (2013).
30. P. A. Gray, W. A. Janczewski, N. Mellen, D. R. McCrimmon, J. L. Feldman, Normal breathing requires preBötzinger complex neurokinin-1 receptor-expressing neurons. *Nat. Neurosci.* **4**, 927–930 (2001).
31. S. M. Winter *et al.*, Glycinergic interneurons are functionally integrated into the inspiratory network of mouse medullary slices. *Pflugers Arch.* **458**, 459–469 (2009).
32. Y. Cui *et al.*, Defining preBötzinger complex rhythm- and pattern-generating neural microcircuits in vivo. *Neuron* **91**, 602–614 (2016).
33. A. Doi, J. M. Ramirez, Neuromodulation and the orchestration of the respiratory rhythm. *Respir. Physiol. Neurobiol.* **164**, 96–104 (2008).
34. J. O. Ramírez-Jarquín *et al.*, Somatostatin modulates generation of inspiratory rhythms and determines asphyxia survival. *Peptides* **34**, 360–372 (2012).
35. R. P. de Sousa Abreu, E. Bondarenko, J. L. Feldman, Phase- and state-dependent modulation of breathing pattern by preBötzinger complex somatostatin expressing neurons. *J. Physiol.* **600**, 143–165 (2022).
36. J. Bouvier *et al.*, Hindbrain interneurons and axon guidance signaling critical for breathing. *Nat. Neurosci.* **13**, 1066–1074 (2010).
37. P. A. Gray *et al.*, Developmental origin of preBötzinger complex respiratory neurons. *J. Neurosci.* **30**, 14883–14895 (2010).
38. P. A. Gray, Transcription factors define the neuroanatomical organization of the medullary reticular formation. *Front. Neuroanat.* **7**, 7 (2013).
39. M. C. D. Picardo, K. T. Weragalaarachchi, V. T. Akins, C. A. Del Negro, Physiological and morphological properties of Dbx1-derived respiratory neurons in the pre-Botzinger complex of neonatal mice. *J. Physiol.* **591**, 2687–2703 (2013).
40. J. P. Kessler, A. Jean, Identification of the medullary swallowing regions in the rat. *Exp. Brain Res.* **57**, 256–263 (1985).
41. A. Amirali, G. Tsai, N. Schrader, D. Weisz, I. Sanders, Mapping of brain stem neuronal circuitry active during swallowing. *Ann. Otol. Rhinol. Laryngol.* **110**, 502–513 (2001).
42. A. Jean, M. Dallaporta, Electrophysiologic characterization of the swallowing pattern generator in the brainstem. *GI Motility* **9**, 1–37 (2006).
43. X. Bao, E. B. Wiedner, S. M. Altschuler, Transsynaptic localization of pharyngeal premotor neurons in rat. *Brain Res.* **696**, 246–249 (1995).
44. Q. Sang, R. K. Goyal, Swallowing reflex and brain stem neurons activated by superior laryngeal nerve stimulation in the mouse. *Am. J. Physiol. Gastrointest. Liver Physiol.* **280**, G191–G200 (2001).
45. E. T. Cunningham, Jr., P. E. Sawchenko, Dorsal medullary pathways subserving oromotor reflexes in the rat: Implications for the central neural control of swallowing. *J. Comp. Neurol.* **417**, 448–466 (2000).
46. A. A. Chiang, Obstructive sleep apnea and chronic intermittent hypoxia: A review. *Chin. J. Physiol.* **49**, 234–243 (2006).
47. K. L. Garand, C. Strange, L. Paoletti, T. Hopkins-Rossabi, B. Martin-Harris, Oropharyngeal swallow physiology and swallowing-related quality of life in underweight patients with concomitant advanced chronic obstructive pulmonary disease. *Int. J. Chron. Obstruct. Pulmon. Dis.* **13**, 2663–2671 (2018).
48. B. Martin-Harris, Optimal patterns of care in patients with chronic obstructive pulmonary disease. *Semin. Speech Lang.* **21**, 311–321 (2000).
49. A. J. Garcia, III, *et al.*, Chronic intermittent hypoxia alters local respiratory circuit function at the level of the preBötzinger complex. *Front. Neurosci.* **10**, 4 (2016).
50. S. Teramoto *et al.*, Impaired swallowing reflex in patients with obstructive sleep apnea syndrome. *Chest* **116**, 17–21 (1999).
51. J. S. Valbuza *et al.*, Swallowing dysfunction related to obstructive sleep apnea: A nasal fibroscopy pilot study. *Sleep Breath.* **15**, 209–213 (2011).
52. C. A. Del Negro, G. D. Funk, J. L. Feldman, Breathing matters. *Nat. Rev. Neurosci.* **19**, 351–367 (2018).
53. T. M. Anderson, J.-M. Ramirez, Respiratory rhythm generation: Triple oscillator hypothesis. *F1000 Res.* **6**, 139 (2017).
54. L. Madisen *et al.*, A toolbox of Cre-dependent optogenetic transgenic mice for light-induced activation and silencing. *Nat. Neurosci.* **15**, 793–802 (2012).
55. N. C. Vann, F. D. Pham, K. E. Dorst, and C. A. Del Negro, Dbx1 pre-Bötzinger complex interneurons comprise the core inspiratory oscillator for breathing in unanesthetized adult mice. *eNeuro* **5**, ENEURO.0130-0118.2018 (2018).
56. C. Gestreau, L. Grélot, A. L. Bianchi, Activity of respiratory laryngeal motoneurons during fictive coughing and swallowing. *Exp. Brain Res.* **130**, 27–34 (2000).
57. R. W. Doty, W. H. Richmond, A. T. Storey, Effect of medullary lesions on coordination of deglutition. *Exp. Neurol.* **17**, 91–106 (1967).
58. J. M. Bonis *et al.*, The effects of lesions in the dorsolateral pons on the coordination of swallowing and breathing in awake goats. *Respir. Physiol. Neurobiol.* **175**, 272–282 (2011).
59. T. G. Bautista, M. Dutschmann, Ponto-medullary nuclei involved in the generation of sequential pharyngeal swallowing and concomitant protective laryngeal adduction in situ. *J. Physiol.* **592**, 2605–2623 (2014).
60. T. Sumi, The activity of brain-stem respiratory neurons and spinal respiratory motoneurons during swallowing. *J. Neurophysiol.* **26**, 466–477 (1963).
61. T. Pitts, A. Huff, M. Reed, K. Iceman, N. Mellen, Evidence of intermediate reticular formation involvement in swallow pattern generation, recorded optically in the neonate rat sagittally sectioned hindbrain. *J. Neurophysiol.* **125**, 993–1005 (2021).
62. D. Paydarfar, R. J. Gilbert, C. S. Poppel, P. F. Nassab, Respiratory phase resetting and airflow changes induced by swallowing in humans. *J. Physiol.* **483**, 273–288 (1995).
63. Y. Zheng, T. Umezaki, K. Nakazawa, A. D. Miller, Role of pre-inspiratory neurons in vestibular and laryngeal reflexes and in swallowing and vomiting. *Neurosci. Lett.* **225**, 161–164 (1997).
64. P. W. Davenport, D. C. Bolser, K. F. Morris, Swallow remodeling of respiratory neural networks. *Head Neck* **33** (suppl. 1), S8–S13 (2011).
65. A. Schindler *et al.*, Oropharyngeal dysphagia in patients with obstructive sleep apnea syndrome. *Dysphagia* **29**, 44–51 (2014).
66. A. M. Bhutada, W. A. Broughton, K. L. Focht Garand, Obstructive sleep apnea syndrome (OSAS) and swallowing function-a systematic review. *Sleep Breath.* **24**, 791–799 (2020).
67. T. Kato *et al.*, Subjective oropharyngeal symptoms for abnormal swallowing in Japanese patients with obstructive sleep apnea syndrome: A descriptive questionnaire study. *Cranio* **34**, 95–99 (2016).
68. N. Pizzorni *et al.*, Dysphagia symptoms in obstructive sleep apnea: Prevalence and clinical correlates. *Respir. Res.* **22**, 117 (2021).
69. I. Ghannouchi, R. Speyer, K. Doma, R. Cordier, E. Verin, Swallowing function and chronic respiratory diseases: Systematic review. *Respir. Med.* **117**, 54–64 (2016).
70. E. Levring Jäghagen, K. A. Franklin, A. Isberg, Snoring, sleep apnoea and swallowing dysfunction: A videoradiographic study. *Dentomaxillofac. Radiol.* **32**, 311–316 (2003).
71. V. Jobin *et al.*, Swallowing function and upper airway sensation in obstructive sleep apnea. *J Appl Physiol (1985)* **102**, 1587–1594 (2007).
72. M. A. T. Campanholo *et al.*, Dysphagia in patients with moderate and severe obstructive sleep apnea. *Rev. Bras. Otorrinolaringol. (Engl. Ed.)* **87**, 422–427 (2021).
73. C.-M. Wang, H.-Y. Li, L.-A. Lee, W.-Y. Shieh, S.-W. Lin, Non-invasive assessment of swallowing and respiration coordination for the OSA patient. *Dysphagia* **31**, 771–780 (2016).
74. E. Chiner *et al.*, Association between obstructive sleep apnea and community-acquired pneumonia. *PLoS One* **11**, e0152749 (2016).
75. E. S. Wallace, M. A. Bhutada, W. A. Broughton, D. J. Eckert, and K. Garand, Knowledge, attitudes, and practice patterns of obstructive sleep apnea among speech-language pathologists. *Sleep Breath.*, 10.1007/s11325-021-02481-2 (2021).
76. T. Hirata *et al.*, Identification of distinct telencephalic progenitor pools for neuronal diversity in the amygdala. *Nat. Neurosci.* **12**, 141–149 (2009).
77. National Research Council, *Guide for the Care and Use of Laboratory Animals* (National Academies Press, Washington, DC, 2011), 8th Ed.
78. J. V. Basmajian, G. Stecko, A new bipolar electrode for electromyography. *J. Appl. Physiol.* **17**, 849 (1962).
79. A. Huff, M. Karlen-Amarante, T. Pitts, J. M. Ramirez, Experimental dataset for the article "Optogenetic stimulation of pre-bötzinger complex reveals novel circuit interactions in swallow-breathing coordination. Figshare. 10.6084/m9.figshare.20288577. Deposited 11 July 2022.
80. S. N. King *et al.*, Swallow motor pattern is modulated by fixed or stochastic alterations in afferent feedback. *Front. Hum. Neurosci.* **14**, 112 (2020).
81. M. Marckwald, *The Movements of Respiration and Their Innervation in the Rabbit. With a Supplement on the Relation of Respiration to Deglutition, and on the Question of the Existence of Respiratory Centres in the Spinal Cord* (Blackie & Son, Glasgow, 1888).